A study of visible-blind properties of a SnO_2's nanowires network photodetector

Estacio P. de Araújo*, Adryelle N. Arantes, Ivani M. Costa and Adenilson J. Chiquito

NanOLaB – Departamento de Física – Universidade Federal de São Carlos – Rodovia Washinton Luiz, Km 235- Monjolinho, 13565-905 – São Carlos, São Paulo – Brasil.

*Corresponding: estacio.paiva@gmail.com

Summary: We developed a SnO_2 nanowire network visible-blind ultraviolet (UV) photodetector for applications in fields such as safety systems, exposure control, decontamination processes, among others. Based on the vapor-liquid-solid (VLS) growth method, a SnO_2 nanowire network was synthetized. The sensor was fabricated based on a metal-semicondutor-metal (MSM) structure and Ag paste was used as simple and efficient electrical contact. To understand the visible-blind property two light sources were used: UV (254-365 nm) and VIS (400-900 nm) Lamps. In Current – Voltage measurements, the device under dark and room ambient conditions presented rectifier contacts with different barrier heights; whereas under UV illumination, the barrier heights seem to be aligned. It was observed that the sensor's photoresponse was optimized for UV Light with rise and decay time ~1s and 3s, respectively, and exhibiting an on/off ratio of 42.5; whereas as for the VIS light both times were longer with an on/off ratio of 1.7, both under V = + 0.1 V. These results are highly significant for developing of a visible-blind photodetector.

Recently, Ultraviolet (UV) light photodetectors have been gaining space in aspect of practice and application, assisting humanity and promoting basic science study. Devices that are transparent to visible (VIS) light and respond uniquely to UV and Deep UV light are certainly useful, e.g., they are commonly employed in Solar observation, optical communication and safety systems, such as flame detection [1,2]. Furthermore, the most recent application of these devices can be associated to the quality control of UV Light sources employed in biological environment, which can be used in decontamination processes related to Sars-CoV-2 virus [3,4]. Given that, over the years, UV photodetectors will become an indispensable device.

With nanotecnology's development, new possibilities of devices arose. The nanometric scale enables a better and precise control of physical and chemical parameters, which provided a successful micro and nano electronic market and gave rise to miniaturized devices [5,6]. Semiconductor materials have demonstrated as excellent candidates to build visible-blind UV photodetectors, such as ZnO [7], TiO_2 [8], GaN [9], SnO_2, among others. Their common property is the large optical gap, which is a basic characteristic demanded for the construction of an UV photodetector. Tin Oxide (SnO_2) is an n-type semiconductor characterized by a wide optical band gap ranging from 3.6 eV to 4.08 eV that belongs to the class of TCOs (Transparence Conducting Oxide). When in its quasi one-dimensional (1D) form, sensors based on SnO_2 have presented a quick detection response, reduced dark current, low operating voltage and high selectivity, aspects that are indispensable for a reliable photodetector [10]. Besides its applicability as an UV photodetector, SnO_2 single nanowire or nanowire network devices have proven to be promising as FET devices [11] and appropriate for gas [12], pH [13] and biologic [14] sensing.

Usually, photodetectors' investigation is focused on the detected wavelength and little is highlighted regarding their ability to be blind to other frequencies. For instance, the study of nano structure-based SnO_2 visible-blind photodetectors dates to less than ten years ago, which indicates that there is still a lot to be discussed. Ting Xie *et al* In 2015 obtained visible-blind photodetectors based on SnO_2/CuO nano-heterojunctions, in which SnO_2 thin films were deposited by rf-sputtering with CuO nanoparticles placed onto them. A metal-semicondutor-metal (MSM) structure was assembled and the devices were characterized by a light source of 290 nm, resulting in an on/off ratio of ~592 with a 0.2 V biasing [15]. By 2018, Duo Chen *et al* built a visible-blind quasi-solid-state UV detector based on SnO_2-TiO_2 nano-heterostructure arrays. They made a mixture of polymer and core-shell structure resulting in an electrolytic solution as active layer. A Schottky photodetector structure was assembled with rise time (τ_r) 0.14 s and decay time (τ_d) 0.06 s, under a light source with wavelength and power of 340 nm and 67.4 $\mu W/cm^2$, respectively [16].

In our previous work, using similar SnO_2 nanowire network devices, significant variations of a UV photodetector behavior under direct sun light irradiation were studied. In addition, it was also noted a sensor's performance dependency on the applied electric field [10]. Here we present a study of a SnO_2 nanowire network as visible-blind photodetector. The nanowire network was grown by the VLS growth technique and the device was built based on a MSM structure, with two silver paste electrodes. The device was investigated in the dark, under UV wavelength (UV Light) and Visible wavelength (VIS Light) illumination. In the first condition, the current was found to be of 8 nA with V = +0.1 V. Under illumination, the UV Light and VIS Light provided a I_{On}/I_{Off} ratio of 42.5 and 1.7, respectively. The UV Light presented τ_r and τ_d of 1s and ~3s, whereas 150s and 200s for the VIS Light. Our results display a great visible-blind UV photodetector, miniaturized and with high sensitivity and reproducibility.

Tin dioxide nanowires were synthesized based on the vapor-liquid-solid (VLS) growth method [17]. Thin films of gold (15 Å) were deposited (Edwards 306 coating system) in Si/SiO2 substrates (oxide layer 500 nm thick). The synthesis was carried out in a tube furnace system (Lindberg Blue M), where a high purity Tin powder (0.1g, Aldrich, purity > 99,99%) was placed in an alumina crucible positioned at the center of the furnace and heated to 950°C for 60 min. For the vapor transport to the synthesis region, an Argon/Oxygen mixture with a constant flow of 20/5 sccm (Mass Flow MKS 1149) was maintained along with controlled pressure by a vacuum pump around 350 mbar. As-synthesized products were then examined by scanning electron microscopy (SEM, JEOL JSM 6510, operated at 20 kV), transmission electron microscopy (TEM, FEI Tecnai G2 F20) and X-ray diffraction (XRD, Rigaku D/max-2500, Cu-Kα radiation).

The XDR pattern in Fig. 1(a) depicts the phase composition and synthesis purity. As expected for the tetragonal structure of SnO_2 (a = 4.73 Å e c = 3.18 Å), all diffraction peaks indexed show rutile-like peaks in accordance to JCPDS Card No. 41-1445 and no impurity phases were detected, suggesting a high phase purity of the nanowire network. The general morphological aspects of the products were characterized by scanning electron microscopy (SEM) image as presented in Fig. 1(b). We can observe nanowires with rectangular cross-sections and lengths of several micrometers.

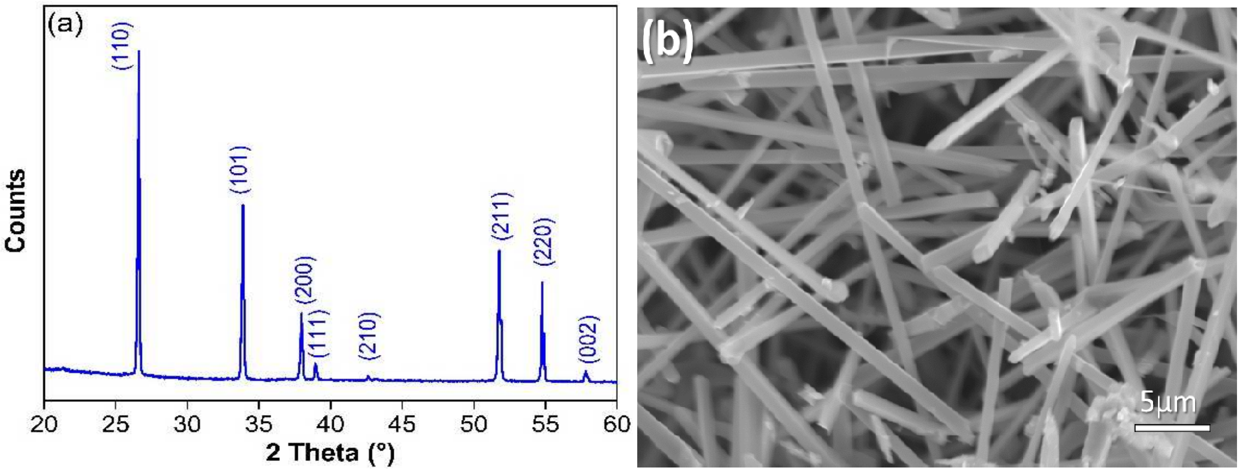

FIG. 1. (a) XDR pattern of the SnO_2 Nanowire network. All the diffraction peaks were index according to the date rutile tetragonal structure SnO_2 (JCPDS Card No. 41-1445). (b) SEM image of the nanowire network.

Through TEM image and its fast-Fourier transform, the morphology was analyzed and the XRD results previously acquired were ratified as follows. Figure 2(a) displays a TEM image of a single NW, presenting the desired morphology for this work. A selected region, Fig. 2(b), shows a HRTEM image indicating that the nanowires are monocrystalline and confirming the sample's high crystalline quality. Figure 2(c) presents the respective Laue pattern, depicting two sets of planes with spacing of 2.64 Å and 2.36 Å, corresponding to (101) and (200) planes, respectively.

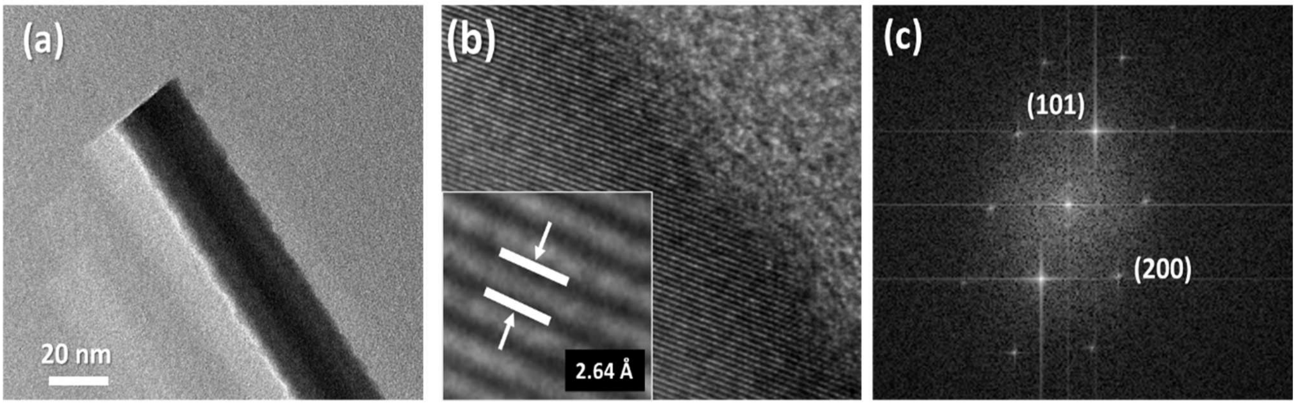

FIG. 2. (a) TEM image exhibits a SnO_2 NW's. (b) HRTEM sets of planes with spacing of 2.64 Å. (c) fast-Fourier transform corresponding to (101) and (200) planes of SnO_2's rutile phase.

The devices were manufactured in a MSM structure [10], in which Ag paste was used as electrical contacts. The fabrication process with Ag paste was chosen due to its high quality mechanical adhesion not only to the nanowires, since it can penetrate into the nanowire network, inset in Fig. 3(a), but also to the external electrical circuit, simplifying the assembly of an integrated circuit [18,19]. Before starting a discussion about the visible-blind photodetector and photoconductivity effect in SnO_2 nanowire network, some details should be discussed. Since a nanowire network contains wires of different sizes and lengths, each one with its value of surface/volume ratio. In addition, the surface states (broken crystal periodicity) can lead to the Fermi pinning on the MS interface, since several different nanowires are in contact with the electrodes, which can modify significantly their transport properties [20]. Therefore, the observed results are the average response of many nanowires being excited. In other words, the electrical response we observe is the randomly percolation pathway chosen by the current to flow from one electrical contact to another, passing through nanowires' homojunctions with different surface/volume ratio [21].

Figure 3(a) - 3(b), depict the Current – Voltage (I-V) curves of a nanowire network device with and without illumination, respectively. In Fig. 3(a) the measurements were performed in the dark and room ambient conditions, the resistance value was found to be approximately of 10^7 Ω. In the Ag/SnO_2 junction, a rectifier behavior arises. Furthermore, one can note that the current for negative biasing is higher than for positive biasing, suggesting the presence of different barrier heights. When under UV illumination, maintaining ambient conditions, a photocurrent effect takes place modifying the behavior. The sensor is exposed to a UV Light source (2 mW/cm^2) with main spectral lines in 254 and 365 nm. Afterwards, it was exposed to a VIS Light (9.5 mW/cm^2), which is coupled to a conventional optical fiber that also acts as an UV filter to avoid any possible contribution from deep blue or even UV wavelengths from the hot filament lamp used. Both sources were positioned 5 cm away from the device. The photocurrent effect can be seen in Fig. 3(b), with resistance of approximately 10^5 Ω for the UV Light and 10^7 Ω for the VIS Light.

When analyzing the results from both sources, one can note that the current significantly increases when the device is under UV Light. Firstly, VIS Light's excitation wavelength can generate mostly transition processes from trapping levels to the conduction band (CB), whereas for the UV Light, the transitions are mainly from the valence band (VB) to the CB. The latter, culminates in an electron-hole (e-h) pair formation and, since the electric field force's strength is greater than the Coulombic forces between e-h pairs, they turn into free carriers improving the conductivity. Figure 3(b) also displays a linear and symmetrical I-V curve, as would be expected for an ohmic behavior between the nanowire network and the silver paste. However, such results do not confirm the absence of barriers and are better understood when the MSM structure is analyzed by a back-to-back diode model [22]. Furthermore, the UV Light can alter the surface states' population and, consequently, the Fermi level. Owing to the Schottky barrier dependence on the Fermi level position, the carriers can then perceive and respond to this lower effective barrier height. When it comes to VIS light, the weak photoresponse, i.e., a small current variation, is attributed to sub bands inside the energy gap, which was already reported for VIS and near infrared excitation of SnO_2 nanowires [23].

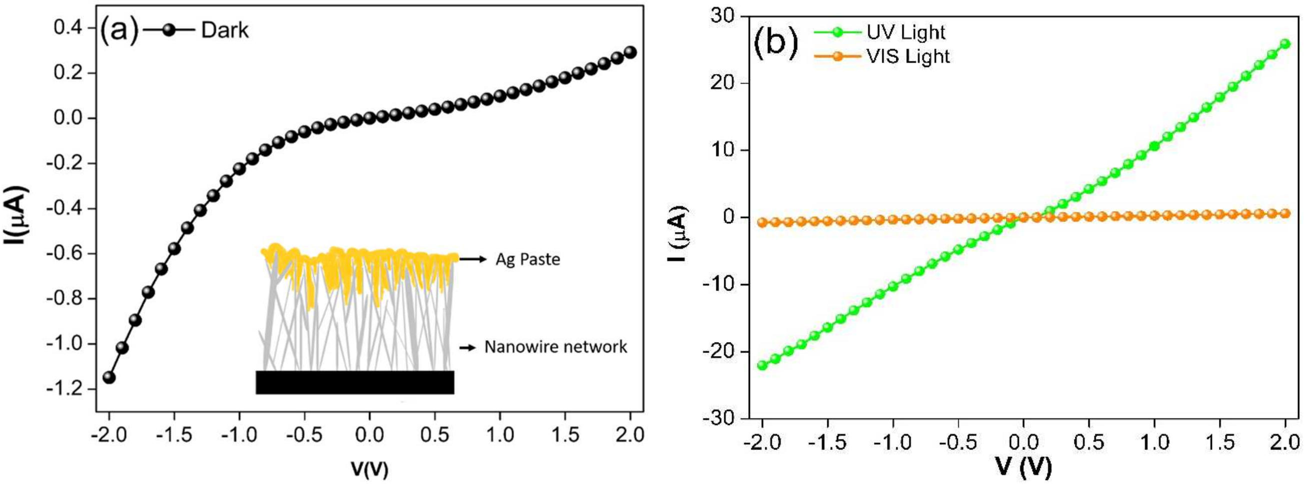

FIG. 3. Current-Voltage (I-V) (a) curve in dark condition and room temperature. (b) Device under different light sources.

Figure 4 shows a sensor's photoresponse. The Current-time (I-t) curves display the behavior of the device under illumination (On) and dark condition (Off). Figure 4(a) depicts the detector's response to UV Light and VIS Light at a + 0.1 V biasing. The On/Off switching was set to 300s. In the first 300 s, the photodetector is in a dark condition and O_2 molecules are adsorbed on the semiconductor's surface, in which I_{Off} ~ 8 nA was measured. Afterwards, at 300 s, the device is exposed to UV and VIS Light. Under UV Light, the current increases quickly reaching a plateau region of 0.34 μA; however, this is not observed for the VIS Light, which resulted in I_{on} ~ 15 nA. Therefore, the I_{On}/I_{Off} ratio calculated for the UV Light and VIS Light are of 42.5 and 1.7, respectively. I_{on} is related to the photoexcited e-h pairs' separation by the external electric field; the electrons of SnO_2's VB interact with light and are excited to the CB contributing to the current, whereas holes can move towards the surface, freeing the Oxygen molecules [24]. After light was turned off, it was observed that the current did not return to its initial value, effect attributed to recombination processes that were not completely over, mainly due to trapping of carriers and adsorbed Oxygen molecules.

Figure 4(b) depicts the normalized time resolved photoresponse of the SnO_2 nanowire network to UV and VIS Light. The τ_r and τ_d were computed, under the UV Light it was obtained τ_r ~1 s and for the VIS Light τ_r ~150 s, whereas τ_d was ~3 s and >300s under the UV Light and VIS Light, respectively. Those differences of τ_r and τ_d time between the Lamps can be attributed to band-to-band recombination that restricts movement of eletrons and holes [25]. Furthermore, even though the VIS Light source's power is considerably higher than the UV one, a low response is detected, which then guarantees not only the device's great sensitivity but also its employment/use as visible-blind photodetectors. The values found for photoconductive gain and transient time were compared to values reported for Ga_2O_3, WO_3 and ZnO [26-28]. Our device was proven reliable, reproductive, with a photocurrent response great enough for practical applicability and easily assembled by an uncomplicated fabrication method.

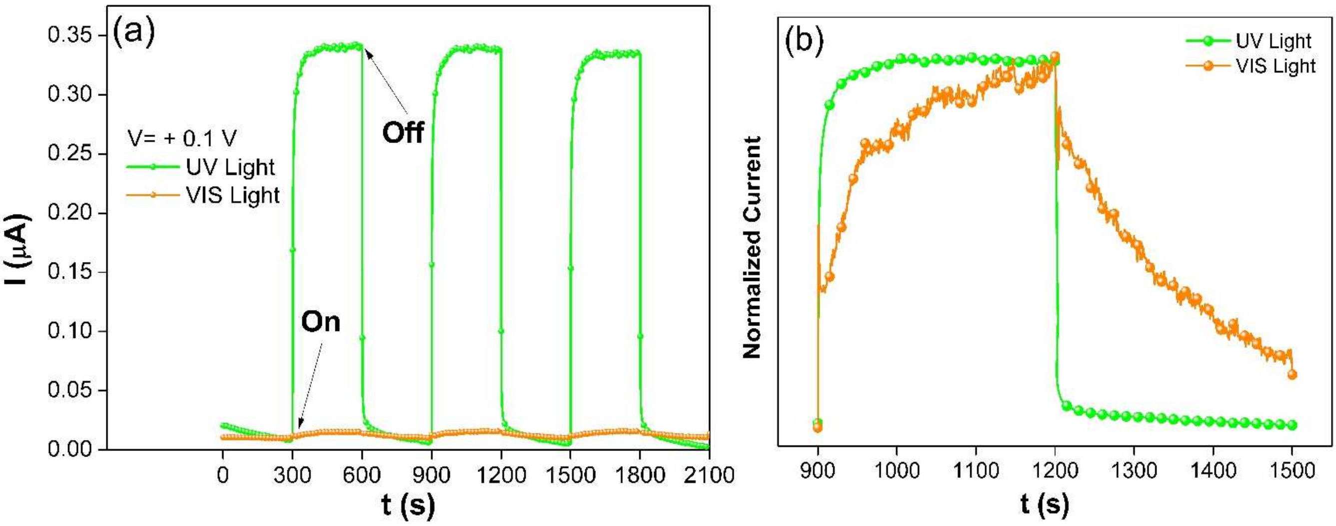

FIG. 4. Current-time (I-t) (a) Time-dependent photocurrent response of the SnO_2 nanowire network. (b) Normalized Current comparison of photocurrent responses.

In summary, a SnO_2 nanowire network visible-blind UV photodetector was built based on the VLS growth technique, which generated a nanowire network of excellent quality. The device has a MSM architecture with a simple and easy process of electrode construction. The sensor operated with rise and decay times of 1 s and ~3 s for the UV Lamp, while VIS Lamp presented extremely longer times for both. The sensitivity was estimated as 42.5 and 1.7 for UV and VIS Lamp, respectively. Our results show that the device has a cut off frequency response, implying that the photodetector responds only to the UV wavelength. Further studies are necessary to fully understand the underlying mechanisms that govern our detectors, the study of the influence of light on the occupation of surface states is necessary. However, the presented results demonstrate that nanowire network SnO_2 are promising materials to fabricate visible-blind photodetectors.

The authors thank the financial support from the Brazilian agencies: Grant Nos. 2013/19692-0, 2013/07296-2, São Paulo Research Foundation (FAPESP) and Grant Nos. 302640/2010-0 and 305615/2014-9 (CNPq).

Data Availability

The data that support the finding of this study are available from the corresponding author upon reasonable request.

References

[1] Tsai, DS., Lien, WC., Lien, DH. et al. Solar-Blind Photodetectors for Harsh Electronics. Sci Rep 3, 2628 (2013). https://doi.org/10.1038/srep02628

[2] Franck Omnès, Eva Monroy, Elias Muñoz, Jean-Luc Reverchon, "Wide bandgap UV photodetectors: a short review of devices and applications," Proc. SPIE 6473, Gallium Nitride Materials and Devices II, 64730E (8 February 2007); https://doi.org/10.1117/12.705393.

[3] Goldust M, Abdelmaksoud A, Navarini AA. Hand disinfection in the combat against COVID-19. J Eur Acad Dermatol Venereol. 2020;34(9):e454-e455. doi:10.1111/jdv.16574

[4] Türsen Ü, Türsen B, Lotti T. Ultraviolet and COVID-19 pandemic. J Cosmet Dermatol. 2020;19(9):2162-2164. doi:10.1111/jocd.13559

[5] H. Chen, K. Liu, L. Hu, A.A. Al-Ghamdi, X. Fang, New concept ultraviolet photodetectors, Mater. Today. 18 (2015) 493–502. https://doi.org/10.1016/j.mattod.2015.06.001.

[6] L. Peng, L. Hu, X. Fang, Low-dimensional nanostructure ultraviolet photodetectors, Adv. Mater. 25 (2013) 5321–5328. https://doi.org/10.1002/adma.201301802.

[7] Leung, Y. H. et al. "ZnO nanowires array p-n homojunction and its application as a visible-blind ultraviolet photodetector." Applied Physics Letters 96 (2010): 053102. https://doi.org/10.1063/1.3299269

[8] tsung-Ying, Tsai & Weng, Wen-Yin & Hsu, Cheng-Liang & Wang, Sin-Hui & Chiu, C. & Hsueh, Ting-Jen & Chang, Sheng-Po. (2012). A Visible-Blind TiO2 Nanowire Photodetector. Journal of The Electrochemical Society. 159. J132-J135. https://doi.org/10.1149/2.008205jes

[9] De Luna Bugallo, Andres & Tchernycheva, Maria & Jacopin, Gwénolé & Rigutti, Lorenzo & Francois, Julien & Chou, Shu-Ting & Lin, Yuan-Ting & Tseng, Po-Han & Tu, Li-Wei. (2010). Visible-blind photodetector based on p-i-n junction GaN nanowire ensembles. Nanotechnology. https://doi.org/10.1088/0957-4484/21/31/315201

[10] Araújo, Estácio & Arantes, Adryelle & Costa, Ivani & Chiquito, Adenilson. (2019). Reliable Tin dioxide based nanowire networks as ultraviolet Solar radiation sensors. Sensors and Actuators A: Physical. 302. https://doi.org/10.1016/j.sna.2019.111825

[11] Adryelle N. Arantes, Estácio P. Araújo, Manuela Pellegrini, André A. Pedersoli, Adenilson J. Chiquito. A simple band model for ultraviolet induced ambipolarity in single SnO2 nanowire devices. Physica E: Low-dimensional Systems and Nanostructures, Volume 128, 2021, 114607, ISSN 1386-9477, https://doi.org/10.1016/j.physe.2020.114607.

[12] Z. Ying, Q. Wan, Z.T. Song, S.L. Feng, SnO2 nanowhiskers and their ethanol sensing characteristics, Nanotechnology. 15 (2004) 1682–1684. https://doi.org/10.1088/0957-4484/15/11/053.

[13] Y. Cheng, P. Xiong, C.S. Yun, G.F. Strouse, J.P. Zheng, R.S. Yang, Z.L. Wang, Mechanism and optimization of pH sensing using SnO 2 nanobelt field effect transistors, Nano Lett. 8 (2008) 4179–4184. https://doi.org/10.1021/nl801696b.

[14] Amorim, Cleber & Blanco, Kate & Costa, Ivani & Araújo, Estácio & Arantes, Adryelle & & Contiero, Jonas & Chiquito, Jobanny. (2020). A New Possibility for Fermentation Monitoring by Electrical Driven Sensing of Ultraviolet Light and Glucose. Biosensors. 10. 97. https://doi.org/10.3390/bios10080097

[15] Xie, Ting & Hasan, Md Rezaul & Qiu, Botong & Arinze, Ebuka & Nguyen, Nhan & Motayed, Abhishek & Thon, Susanna & Debnath, Ratan. (2015). High-performing visible-blind photodetectors based on SnO2/CuO nanoheterojunctions. Applied Physics Letters. 107. https://doi.org/10.1063/1.4938129

[16] Chen, Duo & Wei, Lin & Meng, Lingpan & Wang, Dong & Chen, Yanxue & Tian, Yufeng & Yan, Shishen & Mei, Liangmo & Jiao, Jun. (2018). Visible-blind quasi-solid-state UV detector based on SnO 2 -TiO 2 nanoheterostructure arrays. Journal of Alloys and Compounds. 751. https://doi.org/10.1016/j.jallcom.2018.04.122

[17] I.M. Costa, Y.N. Colmenares, P.S. Pizani, E.R. Leite, A.J. Chiquito, Sb doping of VLS synthesized SnO2 nanowires probed by Raman and XPS spectroscopy, Chem. Phys. Lett. 695 (2018) 125–130. https://doi.org/10.1016/j.cplett.2018.02.014.

[18] Hossein-Babaei, Faramarz & Moghadam, Saeed & Masoumi, Saeed. (2015). Forming ohmic Ag/SnO2 contacts. Materials Letters. 141. 141-144. https://doi.org/10.1016/j.matlet.2014.11.046

[19] Integrated nanoscale electronics and optoelectronics: Exploring nanoscale science and technology through semiconductor nanowires - Pure Appl. Chem., Vol. 76, No. 12, pp. 2051–2068, 2004. DOI: https://doi.org/10.1351/pac200476122051

[20] Direct Measurements of Fermi Level Pinning at the Surface of Intrinsically n-Type InGaAs Nanowires; Nano Lett. 2016, 16, 5135-5142. DOI: 10.1021/acs.nanolett.6b02061

[21] A.L.R. Melzi, A.J. Chiquito, The interplay between Arrhenius and hopping conduction mechanisms in a percolating nanowire network, J. Phys. D. Appl. Phys. 49 (2016). https://doi.org/10.1088/0022-3727/49/31/315303.

[22] A.J. Chiquito, C.A. Amorim, O.M. Berengue, L.S. Araujo, E.P. Bernardo, E.R. Leite, Back-to-back Schottky diodes: The generalization of the diode theory in analysis and extraction of electrical parameters of nanodevices, J. Phys. Condens. Matter. 24 (2012). https://doi.org/10.1088/0953-8984/24/22/225303.

[23] Ate, Abdelrahim & Tang, Zhenan. (2014). Ultrafast and High Sensitive UV/IR Photodetector Based on a Single SnO2 Nanowire. International Journal of Optomechatronics. 4. 6-10. https://doi.org/10.1039/C6TC02420C

[24] Ivani M. Costa, Estácio P. de Araujo, Adryelle N. Arantes, Maria A. Zaghete and Adenilson J. Chiquito. Unusual effects of nanowire-nanowire junctions on the persistent photoconductivity in SnO2 nanowire network devices Nanotechnology 32, 015702 (2021); https://doi.org/10.1088/1361-6528/abb7b2

[25] J A Garrido, E Monroy, I Izpura and E Munoz, Photoconductive gain modelling of GaN photodetectors. Semicond. Sci. Technol. 13 (1998) 563–568. https://doi.org/10.1088/0268-1242/13/6/005

[26] Miaomiao Zhang, Shuai Kang, Liang Wang, Kun Zhang, Yutong Wu, Shuanglong Feng, and Wenqiang Lu. Facile synthesis of β–Ga2O3 nanowires network for solar-blind ultraviolet photodetector. Journal of Physics D: Applied Physics 17, 54 175106 (2021). https://doi.org/10.1088/1361-6463/abe15a

[27] Huang, Kai & Zhang, Qing & Yang, Feng. (2010). Ultraviolet Photoconductance of a Single Hexagonal WO3 Nanowire. Nano Research. 3. 281-287. 10.1007/s12274-010-1031-3. DOI 10.1007/s12274-010-1031-3

[28] Forat H. Alsultany, Z. Hassan, Naser M. Ahmed. A high-sensitivity, fast-response, rapid-recovery UV photodetector fabricated based on catalyst-free growth of ZnO nanowire networks on glass substrate, Optical Materials, Volume 60, 2016, Pages 30-37, ISSN 0925-3467, https://doi.org/10.1016/j.optmat.2016.07.004.